

# Current Helicity and Twist as Two Indicators of the Mirror Asymmetry of Solar Magnetic Fields

D. Sokoloff · H. Zhang · K.M. Kuzanyan ·  
V.N. Obridko · D.N. Tomin · V.N. Tutubalin

Received: 13 April 2007 / Accepted: 7 January 2008 / Published online: 3 February 2008  
© Springer Science+Business Media B.V. 2008

**Abstract** A comparison between the two tracers of magnetic field mirror asymmetry in solar active regions – twist and current helicity – is presented. It is shown that for individual active regions these tracers do not possess visible similarity but averaging by time over the solar cycle, or by latitude, reveals similarities in their behavior. The main property of the data set is antisymmetry over the solar equator. Considering the evolution of helical properties over the solar cycle we find signatures of a possible sign change at the beginning of the cycle, though more systematic observational data are required for a definite confirmation. We discuss the role of both tracers in the context of solar dynamo theory.

**Keywords** Solar activity · Solar magnetic fields

## 1. Introduction

Contemporary astronomical observations suggest two proxies for mirror asymmetry in solar active regions, namely, the current helicity and twist of magnetic field. Both proxies, averaged over a suitable part of active regions, have been measured recently for several hundred

---

D. Sokoloff · H. Zhang · K.M. Kuzanyan (✉)  
National Astronomical Observatories, Chinese Academy of Sciences, Beijing 100012, China  
e-mail: kuzanyan@izmiran.ru

D. Sokoloff  
Department of Physics, Moscow State University, Moscow 119992, Russia

K.M. Kuzanyan · V.N. Obridko  
IZMIRAN, Troitsk, Moscow Region 142190, Russia

K.M. Kuzanyan  
School of Mathematics, University of Leeds, Leeds LS2 9JT, UK

D.N. Tomin · V.N. Tutubalin  
Department of Mechanics and Mathematics, Moscow State University, Moscow 119992, Russia

active regions over more than one solar cycle (see, *e.g.*, Bao and Zhang, 1998, and references therein). Both proxies demonstrate, to some extent, an antisymmetry with respect to the solar equator as well as a cyclic behavior on time scales of the solar activity cycle as traced by sunspots.

Solar magnetic field structure is complicated enough to allow many proxies for its mirror asymmetry, which may not necessarily be proportional to one another. As is natural to expect, current helicity and twist have no simple relation between each other.

A detailed comparison between current helicity and twist as two proxies of the mirror asymmetry of the solar magnetic field is interesting in the context of solar dynamo theory; the key driver of the solar dynamo suggested by Parker (1955) is the  $\alpha$  effect originating in the mirror asymmetry of solar convection and magnetic fields. Proxies of mirror asymmetry of the magnetic field in solar active regions provide a unique observational approach for the direct verification and observation of the  $\alpha$  effect. The link between the  $\alpha$  effect and the proxies under discussion is usually given in terms of the current helicity (*e.g.*, Kleeorin *et al.*, 2003). It would however be risky to insist that solar dynamo theory is well developed enough to disregard twist as an alternative tracer of the  $\alpha$  effect. A conventional mean-field description of the  $\alpha$  effect deals with quantities averaged over substantial temporal or spatial domains rather than over an individual active region. If the similarity of current helicity and twist as tracers of mirror asymmetry becomes more pronounced after averaging, it means that both proxies are reasonable tracers of the  $\alpha$  effect and support the conventional concept of the solar dynamo.

In the present paper we compare current helicity and twist data. First, we study the proxies for an individual active region to demonstrate that the correlation between current helicity and twist is rather weak. Then we demonstrate that the similarity becomes much more pronounced after temporal or spatial averaging.

Our investigation is based on data obtained at the Huairou Solar Observing station of the National Observatories of China (Zhang and Bao, 1998). A previous analysis of current helicity and twist based on these data was presented by Zhang, Bao, and Kuzanyan (2002); see also Kuzanyan, Bao, and Zhang (2000). Here we use a larger data set and improve the statistical analysis, as well as embed the study in the context of the solar dynamo in a more explicit form.

The paper is organized as follows. We briefly review the concepts of current helicity and twist as they are exploited in theoretical studies and give their observational proxies (Section 2). Then we describe the observational data set (Section 3), compare the current helicity and twist for a particular active region (Section 4), and then present the data after temporal or spatial averaging (Section 5). Section 6 contains a more detailed analysis of the antisymmetry of the proxies with respect to the solar equator. We discuss the consequences for solar dynamo theory from this analysis in Section 7.

## 2. Current Helicity and Twist and the $\alpha$ Effect

The conventional parametrization of the magnetic contribution to the  $\alpha$  effect (*e.g.*, Kleeorin and Rogachevskii, 1999) is based on the current helicity  $\chi^c = (\mathbf{b} \cdot \mathbf{j})$ , where  $\mathbf{j} = \text{curl } \mathbf{b}$  is the electric current and  $\mathbf{b}$  is the (small-scale) magnetic field. Because  $\text{curl } \mathbf{b}$  is calculated from the surface magnetic field distribution, the only electric current component that can be derived is  $(\text{curl } \mathbf{b})_z$ . As a consequence of these restrictions, the observable quantity is

$$H_c = \langle b_z (\text{curl } \mathbf{b})_z \rangle, \quad (1)$$

where  $x, y, z$  are local Cartesian coordinates connected with a point on the solar surface, and the  $z$ -axis is normal to the surface (Bao and Zhang, 1998; see also Abramenko, Wang, and Yurchishin, 1997; Pevtsov, Canfield, and Metchalf, 1994). In the framework of the hypothesis of local homogeneity and isotropy this value is  $1/3$  of the current helicity  $\chi^c$ .

Observations (*e.g.*, Zhang and Bao, 1998) provide another proxy for the mirror asymmetry of the magnetic field, that is, twist (Woltjer, 1958), which comes from studies of magnetic fields in the solar atmosphere, where conductivity is high. However, because of the low-beta condition the magnetic field can be described as force-free. Furthermore, according to Maxwell's equations, the magnetic field is a Beltrami field (*i.e.*,  $\text{curl } \mathbf{b} = \alpha_{\text{ff}} \mathbf{b}$ , where the parameter  $\alpha_{\text{ff}}$  is the twist). In the solar interior, however, the magnetic field is not a Beltrami field and twist can be understood as  $\alpha_{\text{ff}} = \langle \text{curl } \mathbf{b} \cdot \mathbf{b} / b^2 \rangle$ . Of course, this definition does not coincide with that of the current helicity. The observational equivalent of the quantity  $\alpha_{\text{ff}}$  is the ratio  $\langle j_z / b_z \rangle$ . The notation  $\alpha_{\text{ff}}$  is generally used for twist in the solar physics literature, though it seems rather confusing from the viewpoint of solar dynamo theory. The details of calculation of twist and helicity from magnetographic observational data are given in the literature (*e.g.*, Wang, Ai, and Deng, 1996; Bao and Zhang, 1998; Zhang and Bao, 1998).

### 3. Observational Data

The observational data used in our analysis were obtained at the Huairou Solar Observing station of the National Astronomical Observatories of China. A magnetograph using the Fe I 5324 Å spectral line determines the magnetic field values at the level of photosphere. The data are obtained by using a CCD camera with  $512 \times 512$  pixels over the whole magnetogram. The entire image size is comparable with the size of an active region, which at about  $2 \times 10^8$  m is comparable with the depth of the solar convective zone.

However, the observational technique allows the line-of-sight field component  $b_z$  to be determined with a much higher precision than the transverse components ( $b_x$  and  $b_y$ ). There are a number of other observational difficulties, such as resolving the  $180^\circ$  ambiguity in the direction of transverse field. The observational technique is described in detail by Wang, Ai, and Deng (1996); see also Abramenko, Wang, and Yurchishin (1996).

The observations are restricted to active regions on the solar surface and we obtain information concerning the surface magnetic field and helicity only. Monitoring solar active regions while they are passing near the central meridian of the solar disk enables observers to determine the full surface magnetic field vector. The observed magnetic field is subjected to further analysis to determine the value of  $\text{curl } \mathbf{b}$ .

An observational program to reveal the values of the twist and the current helicity density over the solar surface requires a systematic approach, both to the monitoring of magnetic fields in active regions and to the data reduction, to reduce the impact of noise. This work has been carried out by a number of research groups (*e.g.*, Seehafer, 1990; Pevtsov, Canfield, and Metchalf, 1994; Rust and Kumar, 1996; Abramenko, Wang, and Yurchishin, 1997; Bao and Zhang, 1998; Kuzanyan, Bao, and Zhang, 2000).

In the present work we analyze two systematic data sets of active regions. The first one consists of 422 active regions over the 10 years 1988–1996 (Bao and Zhang, 1998). This set has been used for theoretical analysis and further data reduction by Kuzanyan, Bao, and Zhang (2000), Zhang, Bao, and Kuzanyan (2002, 2006), Kleeorin *et al.* (2003), and Sokoloff *et al.* (2006).

We also analyze a data set that covers the three years at the beginning of solar cycle 23, namely 1998–2000. This data set was discussed earlier by Bao, Ai, and Zhang (2000, 2002)

and contains data for 64 active regions for which all the helical quantities were determined. The new data are obtained by using the same technique and are processed in much the same way as the earlier data set of Bao and Zhang (1998) covering the ten-year period 1988–1997; see also Zhang and Bao (1998). Thereafter, following Sokoloff *et al.* (2006), we merge these two sets of data and henceforth will consider them as a single continuous data set of 486 active regions.

Observational work is ongoing, and much more data are due to be processed shortly (*e.g.*, Xu *et al.*, 2007).

#### 4. Helicity and Twist for a Particular Active Region

We consider both observable parameters for a particular active region as random quantities. The standard way to represent a random quantity is as a histogram presenting the percentage of data lying in a given range. We tried this method and found that the result is not very informative. The point is that our data set is small and the data are quite noisy. So we used a more advanced method and calculated a cumulative distribution function (c.d.f.), which is much more robust than the usual probability distribution function.

Let our set contain  $N$  active regions. For the sake of definiteness consider a given value of  $x = \alpha_{\text{ff}}$  (or  $\chi^c$  if appropriate). Let  $n$  active regions have twist lower than  $x$ . Then the probability for  $\alpha_{\text{ff}}$  to be lower than  $x$  is estimated as  $P = n/N$ . Let  $\xi$  be a Gaussian variable with the same mean value  $\mu$  and standard deviation  $\sigma$  as  $\alpha_{\text{ff}}$  and  $y$  the value for which the probability for  $(\xi - \mu)/\sigma$  to be lower than  $y$  is  $P$ . The results for various  $x$  are shown by dots in  $(x, y)$  coordinates (Figure 1) and can be compared with the c.d.f. for a Gaussian distribution shown by the solid line. We see that the dots (twist) on the upper panel are substantially closer to the straight line than on the lower panel (helicity). We conclude that twist is much closer to a Gaussian random quantity than helicity. Note that the link between both quantities is very nonlinear, and so at least one of the quantities (here the helicity) has to be non-Gaussian.

Next, the twist and helicity of the observational data normalized to their means ( $\mu_{\text{ff}}$  and  $\mu_c$ , correspondingly) and standard deviations ( $\sigma_{\text{ff}}$  and  $\sigma_c$ , correspondingly) are shown on a scatter diagram (Figure 2). If the statistical dependence between the twist and helicity is strong, the cluster of points obtained must form an elongated ellipse. In our case the axes of the ellipse are nearly parallel to the coordinate axes, and a weak correlation can be described by the relation  $(\chi^c - \mu_c)/\sigma_c = 0.006 + 0.1(\alpha_{\text{ff}} - \mu_{\text{ff}})/\sigma_{\text{ff}}$  obtained by the least square method. The resulting correlation may be formally significant; however, this is difficult to confirm because of the non-Gaussian distribution of helicity. Nonetheless, the correlation revealed appears to be robust with respect to discarding data that strongly deviate from the mean. Note, however, that theoretical considerations based on such weak correlations are not very reliable.

For the helicity and twist data obtained over individual active regions, the solar cycle is not well pronounced. As an example, in Figure 3 we show helicity (upper panel) and twist (lower panel) as functions of the cycle phase for active regions in the southern hemisphere. The periodic behavior is hardly visible in either case. Notice that separate presentation of the data for northern and southern hemispheres is required because of the hemispheric rule according to which both tracers tend to have opposite signs in the northern and southern hemispheres. However, appropriate averaging of the data taken over rather narrow temporal or latitudinal intervals indicates similar cyclic behavior for both quantities. This is described in the following section.

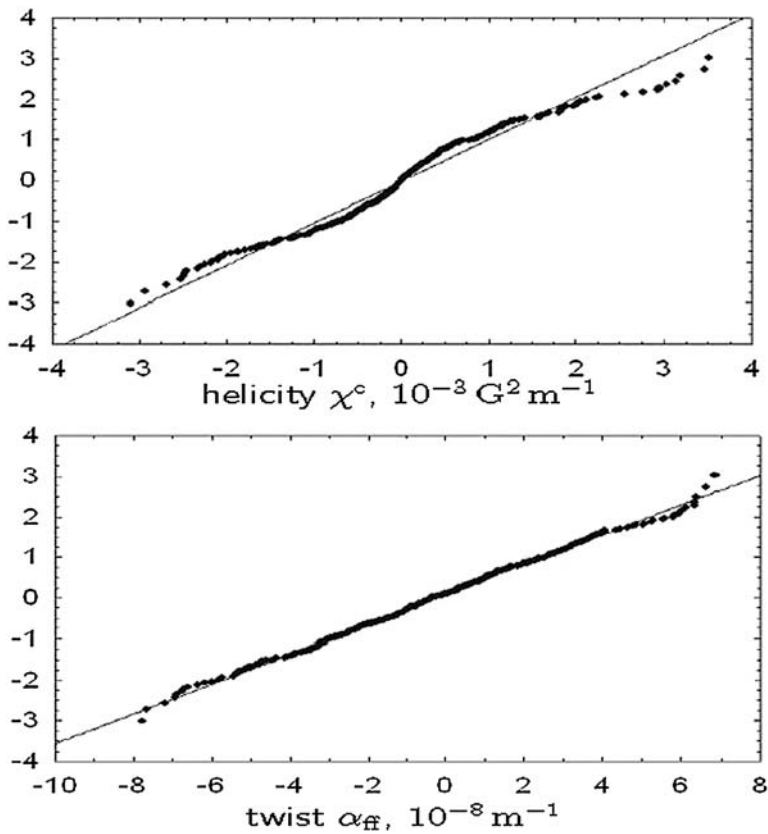


**Figure 1** Cumulative distribution function for the current helicity (upper panel) and twist (lower panel). The first coordinate of the point is the value of the parameter under investigation for a particular active region. The second coordinate is the expected value of the standard deviations for a Gaussian quantity with the same mean and standard deviation that gives the same probability (see text for details). For a Gaussian quantity, we must obtain straight lines, which are also shown on both panels.

## 5. Evolution of the Mean Values over an Activity Cycle

The mean values of the twist and helicity calculated over relatively narrow time or latitudinal intervals behave quite differently. Following Kleeorin *et al.* (2003), we divide the entire data set into two-year time intervals and plot the mean helicity (Figure 4, upper panel) and mean twist (Figure 4, lower panel) for each interval separately for the northern and southern hemispheres. The error boxes are calculated by assuming the quantities are Gaussian. Figure 4 shows that the cyclic variations of the helicity and twist are very similar. Both parameters increase in absolute value in the middle of the cycle and decrease at the beginning and end of the cycle. Both helicity and twist change sign from one hemisphere to another. For both tracers, the cycle is seen more distinctly in the southern hemisphere; the cycle in the northern hemisphere is somewhat better pronounced in helicity than in twist. However, the mean values contain significant uncertainties. Therefore, we cannot confirm the hypothesis that the mirror asymmetry of the magnetic field changes sign in the course of an activity cycle,

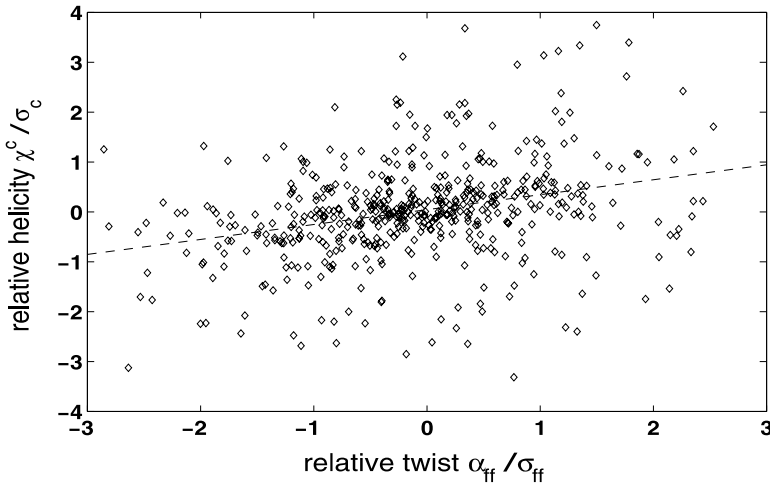


**Figure 2** Scatter diagram for the twist and helicity normalized to the corresponding standard deviations. A correlation between the twist and helicity means that the distribution of points will form an ellipsoid, whose inclination to the coordinate axes provides the correlation coefficient. In the case under discussion, the correlation is seen to be weak, though a trend (shown by a dashed line) is noticeable.

as suggested by Hagino and Sakurai (2005). We have checked that the result is robust with respect to discarding data that strongly deviate from the mean.

Note that, in comparison with Kleorin *et al.* (2003), we use an extended database covering a longer period of observations. The observational database and the procedure providing a synthetic description of a full cycle using partial observations of two successive cycles are given in Sokoloff *et al.* (2006).

A similar picture was obtained by averaging the data over  $5^\circ$  latitudinal bands (Figure 5). Again, both tracers display a mirror asymmetry with respect to the solar equator. The helicity data in the southern hemisphere are more regular than in the northern one, but the twist data seem to be more regular in the northern hemisphere. Also, we do not see polarity inversions over latitudinal bands in either hemisphere. (As shown by the confidence intervals, the apparent polarity reversal at  $-30^\circ$  for helicity is insignificant and disappears if strongly deviating values are discarded.) Notice that a similar result was obtained by Zhang, Bao, and Kuzanyan (2002) using a smaller data set; see their Figure 4.

In general, we conclude that the twist data averaged over time or latitude intervals can be used to determine quite reliably the behavior of the helicity and vice versa.

Isolating the particular time intervals and latitudinal bands and separating the data by hemispheres, we decrease significantly the number of values to be averaged in each case. Therefore, the available data appear to be insufficient for further fragmentation. In particular, butterfly diagrams for the helicity (Sokoloff *et al.*, 2006) and twist (Figure 6) based on these data are merely illustrative and cannot be used directly to draw conclusions on, say, the inversion of the sign of helicity.

Note that a weak correlation between the helicity and twist data for individual active regions discussed in the previous section needs an explanation in the context of the revealed pronounced correlation between their mean values. We may suggest that significant correlation between the helicity and twist for individual active regions calculated in a particular latitudinal range and cycle phase does exist, but this may be disguised by the general cyclic

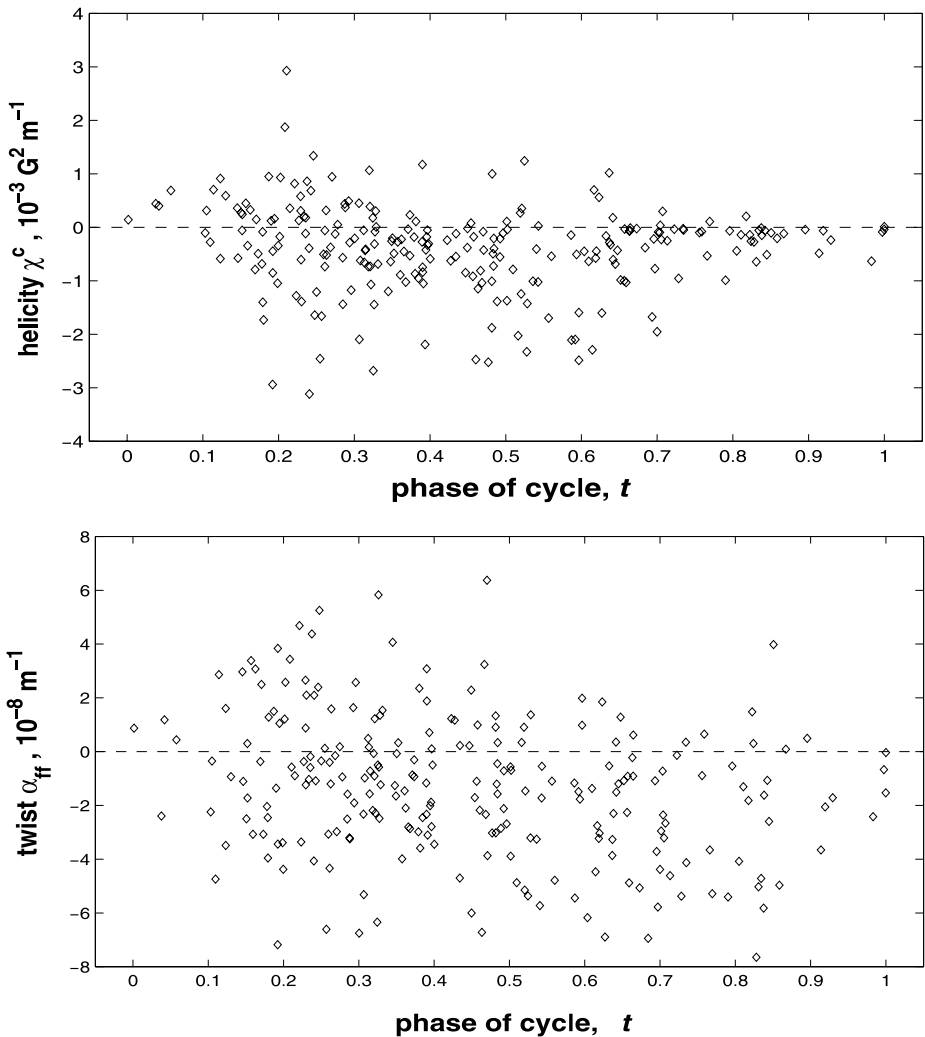


**Figure 3** Helicity (upper panel) and twist (lower panel) for individual active regions as a function of the phase cycle (for the southern hemisphere). The cycle is not pronounced though one can see some predominance of negative values in both helicity parameters, in accord with the polarity law.

dependence of the entire data set, though the limited size of the available data set does not allow us to verify this suggestion.

## 6. Statistics of Active Regions Violating the Polarity Law

Of course, the polarity law for the helicity and twist is not strictly followed. As shown by the helicity and twist measurements in individual active regions, there are many active regions that violate this law. It turns out (Sokoloff *et al.*, 2006) that the active regions in which the current helicity does not obey the polarity law are most frequently observed at the beginning

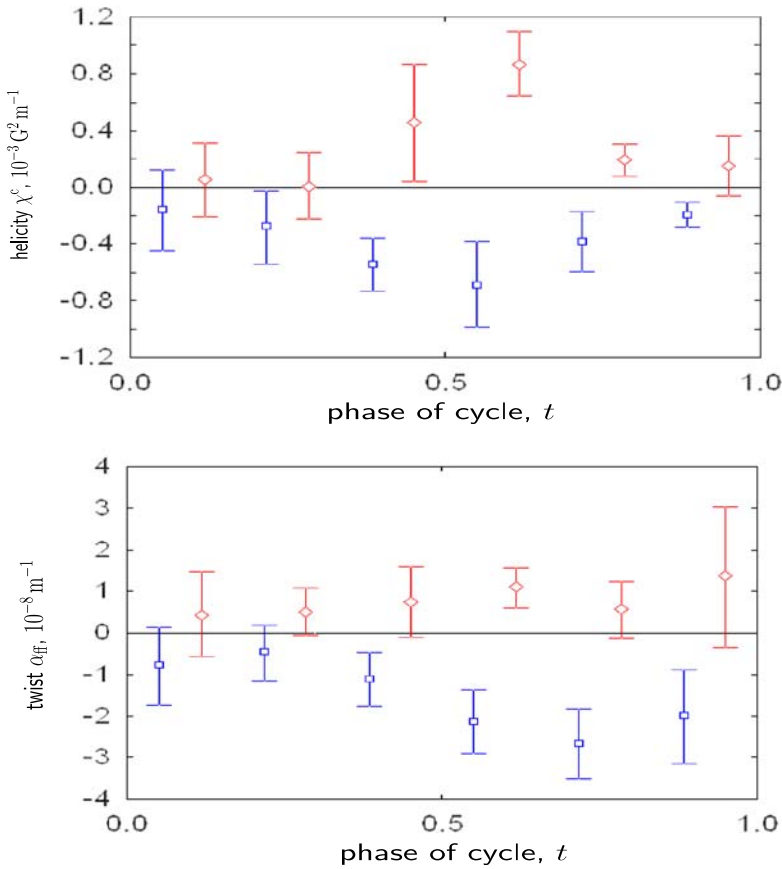


**Figure 4** Two-year-averaged mean helicity (upper panel) and twist (lower panel) values as a function of the cycle phase calculated separately for the northern and southern hemispheres. Blue squares correspond to the northern hemisphere; red diamonds correspond to the southern one. The data points averaged over both hemispheres have been artificially shifted in opposite sides for better performance. One can easily see the polarity law and evolution of both values over the cycle.

of the cycle (*cf.* Tang and Le, 2005). Table 1 presents the corresponding statistics for both the helicity and twist. The tendency of the law-breaking active regions to appear preferably at the beginning of the cycle is noticeable in the case of the twist as well, but this is much weaker than in the case of the helicity, in contrast to what might be expected according to Choudhuri, Chatterjee, and Nandy (2004). This raises a problem that challenges further development of the dynamo theory.

## 7. Discussion

In this paper we have shown that the behavior of current helicity and twist is similar. Both these quantities are obtained from the same distribution of local values of vertical magnetic field  $b_z$  and the electric current  $j_z$ , properly averaged upon calculation. Therefore this similarity is expected but is not evident in advance. One can also suggest other quantities to



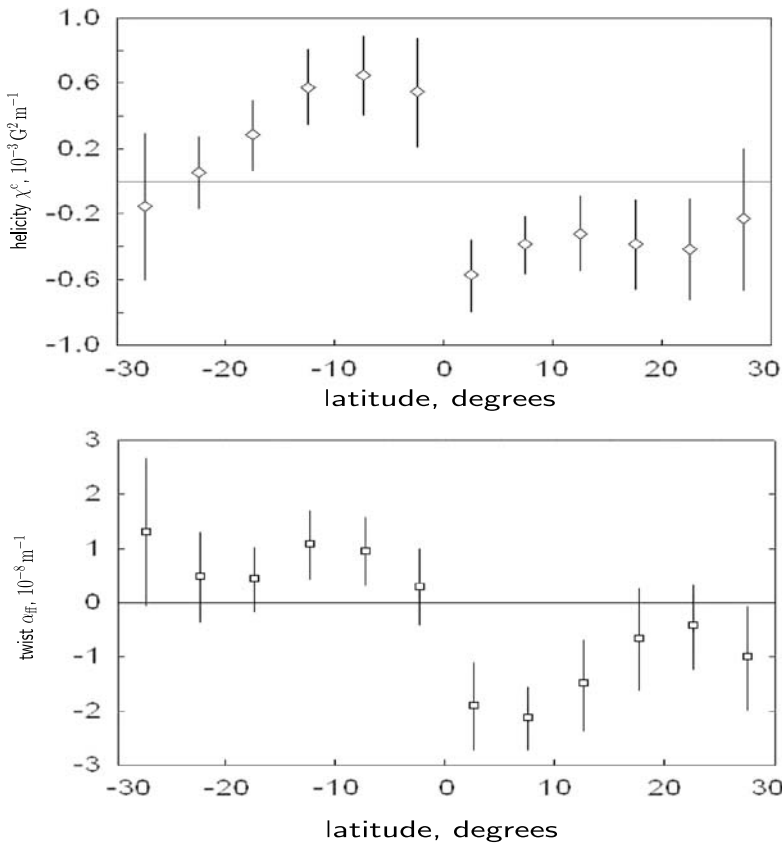


**Figure 5** The helicity (upper panel) and twist (lower panel) values averaged over 5° latitudinal bands. One can easily see the polarity law.

**Table 1** Statistics of active regions breaking the polarity law for the current helicity and the twist. For helicity,  $n_-$  is the number of active regions before the cycle phase  $t$  and  $p$  is the relative number (probability) of the law-breaking active regions. For the twist,  $N_-$  is the active region number and  $\tilde{p}$  is the probability.

$t$	$n_-$	$N_-$	$p$	$\tilde{p}$
0.18	18	16	$54 \pm 8\%$	$48 \pm 18\%$
0.30	60	54	$46 \pm 4\%$	$42 \pm 9\%$
0.43	85	91	$37 \pm 3\%$	$40 \pm 6\%$
0.55	101	123	$32 \pm 2\%$	$38 \pm 5\%$
0.68	112	144	$28 \pm 2\%$	$36 \pm 5\%$
0.80	121	162	$26 \pm 2\%$	$35 \pm 4\%$

be calculated from the same vector magnetographic data set, such as  $\alpha_{\text{best}}$ , which can also be used as a tracer of mirror asymmetry of magnetic fields (see, e.g., Hagino and Sakurai, 2005). We may suggest making comparisons of these related quantities in forthcoming papers.

The analysis here exploits sunspots as tracers of processes in the region of magnetic field generation (i.e., in the region of dynamo action). Let us discuss the applicability of this

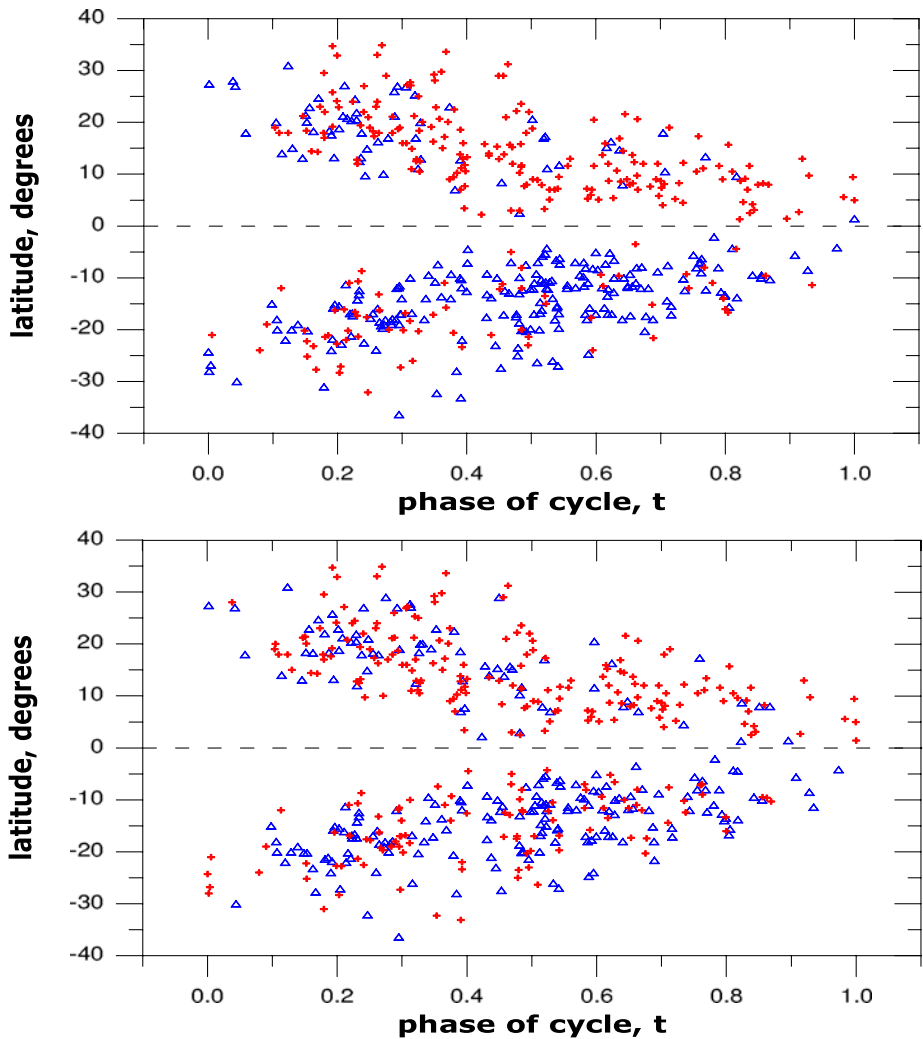


**Figure 6** Butterfly diagrams for the helicity (upper panel) and twist (lower panel). The red crosses mark the positions of the active regions with negative values of the corresponding parameters, and the blue triangles correspond to the positive values. The two diagrams look very similar and so can hardly be distinguished by sight.

approach. At the photospheric level magnetic pressure in sunspots is likely much larger than the gas pressure, and so the magnetic field can be considered in the vacuum approximation. This supports the application of potential magnetic field models for the solar corona and to some extent for the photosphere. Correspondingly, we use twist as a quantity reflecting mirror asymmetry of magnetic field in the potential approximation. The situation becomes quite different in the subphotospheric region as the gas pressure and kinetic energy become comparable with the magnetic energy just below the photosphere. Correspondingly, we use current helicity as a quantity reflecting the mirror asymmetry in the solar interior.

The extent to which the current helicity data taken at the photospheric level represent values for the dynamo region seems to be much more delicate. The point is that time–distance

helioseismology demonstrated that sunspots evanesce only at a depth of 5–10 Mm. One might conclude that this fact precludes using sunspots as tracers of physical processes in the solar interior. We believe that such an opinion would be an exaggeration. First, helioseismology gives the depth of the region with a temperature depression only. Below this depth a temperature excess is expected (Ponomarenko, 1972a, 1972b; Parker, 1974, 1976). It is reasonable to believe that the magnetic field below a sunspot cannot suppress convection even though it is not negligible. According to our modern understanding in the framework of the cluster model, the motion of magnetic flux tubes is rather independent of convective motion. This viewpoint is supported by direct observations (Zhao, Kosovichev, and Duvall, 2004; Gizon, Duvall, and Schou, 2003). In addition, long-term monitoring of sunspot rotation demonstrates a clear solid-body component typical for tachocline motion (Ivanov, 2004). One may expect that sunspots mimic somehow the structure of the large-scale toroidal magnetic fields in the solar interior. Therefore, we may use the data on current helicity and twist as tracers of the dynamo mechanism, though this question requires further clarification.

**Acknowledgements** We would like to thank the anonymous referee for constructive criticism that helped to improve the paper. DS and KK would like to acknowledge support from the Chinese Academy of Sciences and NSFC toward their visits to Beijing under Project Nos. RFBR-NNSFC 05-02-39017 and RFBR 06-05-64619, 05-02-16090, 07-02-00246, and 08-02-00070 and also Leading Schools Grant No. HIII-8499.2006.2. The work was supported by National Basic Research Program of China 2006CB806301, National Natural Science Foundation of China 10611120338, 10473016, 10673016, 60673158, and Important Directional Project of Chinese Academy of Sciences KLCX2-YW-T04. DS is grateful to the Royal Society for financial support of his visit to the United Kingdom. We are grateful to Andrew Fletcher for critical reading of the manuscript.

## References

- Abramenko, V.I., Wang, T.J., Yurchishin, V.B.: 1996, *Solar Phys.* **168**, 75.  
Abramenko, V.I., Wang, T.J., Yurchishin, V.B.: 1997, *Solar Phys.* **174**, 291.  
Bao, S.D., Zhang, H.Q.: 1998, *Astrophys. J.* **496**, L43.  
Bao, S.D., Ai, G.X., Zhang, H.Q.: 2000, *J. Astrophys. Astron.* **21**, 303.  
Bao, S.D., Ai, G.X., Zhang, H.Q.: 2002. In: Rickman, H. (ed.) *IAU Highlights Astron.* **12**, 392.  
Choudhuri, A.R., Chatterjee, P., Nandy, D.: 2004, *Astrophys. J.* **615**, L57.  
Gizon, L., Duvall, T.L. Jr., Schou, J.: 2003, *Nature* **421**, 43.  
Hagino, M., Sakurai, T.: 2005, *Publ. Astron. Soc. Japan* **57**, 481.  
Ivanov, E.V.: 2004. In: Stepanov, A.V., Benevolenskaya, E.E., Kosovichev, A.G. (eds.) *Multi-Wavelength Investigations of Solar Activity*, *IAU Symp.* **223**, 261.  
Kleerorin, N., Rogachevskii, I.: 1999, *Phys. Rev. E* **59**, 6724.  
Kleerorin, N., Kuzanyan, K., Moss, D., Rogachevskii, I., Sokoloff, D., Zhang, H.: 2003, *Astron. Astrophys.* **409**, 1097.  
Kuzanyan, K.M., Bao, S., Zhang, H.: 2000, *Solar Phys.* **191**, 231.  
Parker, E.N.: 1955, *Astrophys. J.* **122**, 293.  
Parker, E.N.: 1974, *Solar Phys.* **36**, 249.  
Parker, E.N.: 1976, *Astrophys. J.* **204**, 259.  
Pevtsov, A.A., Canfield, R.C., Metchalf, T.R.: 1994, *Astrophys. J.* **425**, L117.  
Ponomarenko, Yu.B.: 1972a, *Astron. Rep.* **49**, 148.  
Ponomarenko, Yu.B.: 1972b, *Astron. Rep.* **49**, 568.  
Rust, D.M., Kumar, A.: 1996, *Astrophys. J.* **464**, L119.  
Seehafer, N.: 1990, *Solar Phys.* **125**, 219.  
Sokoloff, D., Bao, S.D., Kleerorin, N., Kuzanyan, K., Moss, D., Rogachevskii, I., Tomin, D., Zhang, H.: 2006, *Astron. Nachr.* **327**, 876.  
Tang, Y.Q., Le, G.M.: 2005. In: Acharya, B.S., Gupta, S., Jagadeesan, P., Jain, A., Karthikeyan, S., Morris, S., Tonwar, S. (eds.) *Proc. 29-th International Cosmic Ray Conference*, **1**, Tata Institute of Fundamental Research, 5.  
Wang, T.J., Ai, G.X., Deng, Y.Y.: 1996, *Publ. Beijing Astron. Obs.* **28**, 31.

- Woltjer, L.: 1958, *Proc. Natl. Acad. Sci. USA* **44**, 489.
- Xu, H., Gao, Y., Zhang, H., Sakurai, T., Pevtsov, A.A., Sokoloff, D.: 2007, *Adv. Space Res.* **39**, 1715.
- Zhang, H., Bao, S.: 1998, *Astron. Astrophys.* **339**, 880.
- Zhang, H., Bao, S., Kuzanyan, K.M.: 2002, *Astron. Rep.* **46**, 414.
- Zhang, H., Sokoloff, D., Rogachevskii, I., Moss, D., Lamburt, V., Kuzanyan, K., Kleeorin, N.: 2006, *Monthly Notices Roy. Astron. Soc.* **365**, 276.
- Zhao, J., Kosovichev, A.G., Duvall, T.L.: 2004, *Astrophys. J.* **607**, L135.